Quark charge balance function and hadronization effects in relativistic heavy ion collisions

Jun Song,[1,2] Feng-lan Shao,[3] and Zuo-tang Liang[2]

[1]*Department of Physics, Jining University, Jining, Shandong 273155, China*
[2]*School of Physics, Shandong University, Jinan, Shandong 250100, China*
[3]*Department of Physics, Qufu Normal University, Shandong 273165, China*

We calculate the charge balance function of the bulk quark system before hadronization and those for the directly produced and the final hadron system in high energy heavy ion collisions. We use the variance coefficient to describe the strength of the correlation between the momentum of the quark and that of the antiquark if they are produced in a pair and fix the parameter by comparing the results for hadrons with the available data. We study the hadronization effects and decay contributions by comparing the results for hadrons with those for the bulk quark system. Our results show that while hadronization via quark combination mechanism slightly increases the width of the charge balance functions, it preserves the main features of these functions such as the longitudinal boost invariance and scaling properties in rapidity space. The influence from resonance decays on the width of the balance function is more significant but it does not destroy its boost invariance and scaling properties in rapidity space either. The balance functions in azimuthal direction are also presented.

I. INTRODUCTION

The electric charge balance function for the final state hadrons has been proposed as a probe to study the properties of the bulk matter system produced in relativistic heavy ion collisions [1–7]. Measurements have already been carried out both in the rapidity space [8–10] and in the azimuthal direction [11]. From the data now available [10,11], we are already able to see clearly that the charge balance functions for hadrons produced in high energy heavy ion collisions are significantly narrower than those for pp collisions at the same energies and they are narrower for central collisions than those for peripheral collisions, indicating a strong local charge compensation in the bulk quark matter system produced in heavy ion collisions. The data [12] further show that the charge balance functions have the longitudinal boost invariance and scaling properties in the rapidity space, and these properties hold for either transverse momentum p_T-integrated balance functions or those for different p_T ranges.

These features of the experimental data [10–12] are rather striking and suggest that such studies should be able to give more insights to the understanding of the properties of the bulk quark matter system produced in AA collisions. It is thus natural to ask whether such behavior hold also for the quark antiquark system before hadronization. It is also important to see how large the influence from the hadronization and resonance decay.

In this paper, we propose a simple working model to calculate the charge balance function for the bulk quark antiquark system before hadronization. We introduce the variance coefficient ρ to describe the local correlation in the momentum distribution for the quark and that for the antiquark if they are produced in a pair. The parameter ρ measures the strength of the quark-antiquark momentum correlation produced in the processes. We study the influence due to hadronization process including the contributions due

to resonance decay by simulating the hadronization process using a quark combination model which describe the final hadron distributions.

The paper is organized as follows. In Sec. II, we study the charge balance of the quark system before hadronization. In Sec. III, we study the charge balance function of initial hadron system as well as final hadron system, and compare them with that of quark system. Section IV gives a brief summary.

II. CHARGE BALANCE FUNCTION OF THE SYSTEM OF QUARKS AND ANTIQUARKS

We recall that the balance function is in general defined as [1]

$$B(\Delta_2|\Delta_1) = \tfrac{1}{2}\{\rho(b, \Delta_2|a, \Delta_1) - \rho(a, \Delta_2|a, \Delta_1) \\ + \rho(a, \Delta_2|b, \Delta_1) - \rho(b, \Delta_2|b, \Delta_1)\}, \quad (1)$$

where $\rho(b, \Delta_2|a, \Delta_1)$ is the conditional probability of observing a particle of type b in bin Δ_2 given the existence of a particle of type a in bin Δ_1. The label a may, e.g., refer to all positively charged particles while b refers to all negatively charged ones; a may also refer to all particles with strangeness -1 while b refers to those with $+1$, and so on. For a system consisting of many particles, the conditional probability $\rho(b, \Delta_2|a, \Delta_1)$ is calculated by counting the number $N(b, \Delta_2|a, \Delta_1)$ of the ab pairs where a is in bin Δ_1 and b is in bin Δ_2 and the number $N(a, \Delta_1)$ of a in bin Δ_1, i.e.,

$$\rho(b, \Delta_2|a, \Delta_1) = \frac{N(b, \Delta_2|a, \Delta_1)}{N(a, \Delta_1)}. \quad (2)$$

These numbers can be calculated using the usual two-particle joint momentum distribution function $f_{ab}(\boldsymbol{p}_1, \boldsymbol{p}_2)$ and single particle distribution function $f_a(\boldsymbol{p})$ or $f_b(\boldsymbol{p})$, respectively.

They are given by

$$N(b, \Delta_2 | a, \Delta_1) = \int_{\Delta_1} d^3 p_1 \int_{\Delta_2} d^3 p_2 \, f_{ab}(\boldsymbol{p}_1, \boldsymbol{p}_2), \quad (3)$$

$$N(a, \Delta_1) = \int_{\Delta_1} d^3 p_1 \, f_a(\boldsymbol{p}_1). \quad (4)$$

We see that, if a is locally compensated by b, the balance function $B(\Delta_2 | \Delta_1)$ should have a very narrow distribution. In the opposite case, it should be flat. The balance function is normalized to unity, i.e., $\sum_{\Delta_2} B(\Delta_2 | \Delta_1) = 1$.

A. A working model for the two particle joint momentum distribution functions in the bulk quark matter system

We consider the bulk quark matter system produced in heavy ion collisions at high energies. We suppose that the system is composed of N_q quarks and $N_{\bar{q}}$ antiquarks. We denote the normalized momentum distribution of the quarks and antiquarks by $n_q(\boldsymbol{p})$ and $n_{\bar{q}}(\boldsymbol{p})$, respectively. In heavy ion collisions, the bulk matter system consists of new created quarks, antiquarks, and the quarks from the incident nuclei. Those quarks from the incident nuclei are referred as the net quarks and the new born quarks and antiquarks are created in pairs.

To obtain a charge balance function that is narrower than that for the completely uncorrelated case, we introduce a minimum correlation in the two particle joint momentum distributions in the system. To this end, we construct the following working model for the two particle joint momentum distribution for the bulk quark matter system. We assume that there is no correlation between the momentum distributions of two different quarks or two antiquarks. The joint distributions are simply the products of the corresponding single particle momentum distributions, i.e.,

$$f_{q_1 q_2}(\boldsymbol{p}_1, \boldsymbol{p}_2) = N_{q_1} N_{q_2} n_{q_1}(\boldsymbol{p}_1) n_{q_2}(\boldsymbol{p}_2) \left(1 - \delta_{q_1, q_2}\right)$$
$$+ N_{q_1}(N_{q_2} - 1) n_{q_1}(\boldsymbol{p}_1) n_{q_2}(\boldsymbol{p}_2) \delta_{q_1, q_2}, \quad (5)$$

$$f_{\bar{q}_1 \bar{q}_2}(\boldsymbol{p}_1, \boldsymbol{p}_2) = N_{\bar{q}_1} N_{\bar{q}_2} n_{\bar{q}_1}(\boldsymbol{p}_1) n_{\bar{q}_2}(\boldsymbol{p}_2) \left(1 - \delta_{q_1, q_2}\right)$$
$$+ N_{\bar{q}_1}(N_{\bar{q}_2} - 1) n_{\bar{q}_1}(\boldsymbol{p}_1) n_{\bar{q}_2}(\boldsymbol{p}_2) \delta_{q_1, q_2}, \quad (6)$$

where q_1 and q_2 denote the flavors of the quarks. For the $q\bar{q}$ joint momentum distribution, we introduce a correlation between the moment distribution of the quark and that of the antiquark which are produced in the same pair. In this case, the joint distribution for a quark q_1 and an antiquark q_2 is given by

$$f_{q_1 \bar{q}_2}(\boldsymbol{p}_1, \boldsymbol{p}_2) = N_{q_1} N_{\bar{q}_2} n_{q_1}(\boldsymbol{p}_1) n_{\bar{q}_2}(\boldsymbol{p}_2)$$
$$+ N_{\bar{q}_1} \left[n_{q\bar{q}}^{\text{pair}}(\boldsymbol{p}_1, \boldsymbol{p}_2) - n_{\bar{q}_1}(\boldsymbol{p}_1) n_{\bar{q}_2}(\boldsymbol{p}_2) \right] \delta_{q_1, q_2}. \quad (7)$$

The single-particle momentum distributions are related to $n_{q\bar{q}}^{\text{pair}}(\boldsymbol{p}_1, \boldsymbol{p}_2)$ by

$$n_{\bar{q}}(\boldsymbol{p}_2) = \int d^3 p_1 n_{q\bar{q}}^{\text{pair}}(\boldsymbol{p}_1, \boldsymbol{p}_2), \quad (8)$$

$$n_q(\boldsymbol{p}) = \frac{N_{\bar{q}}}{N_q} n_{\bar{q}}(\boldsymbol{p}) + \frac{N_{\text{net}}}{N_q} n_{\text{net}}(\boldsymbol{p}). \quad (9)$$

Hence, as long as we know $n_{q\bar{q}}^{\text{pair}}(\boldsymbol{p}_1, \boldsymbol{p}_2)$ and $n_{\text{net}}(\boldsymbol{p})$, we can calculate the two particle joint momentum distributions for the qq, $\bar{q}\bar{q}$, and $q\bar{q}$ systems.

To calculate $n_{q\bar{q}}^{\text{pair}}(\boldsymbol{p}_1, \boldsymbol{p}_2)$, we adopt the picture of the hydrodynamic theory. Here, we assume the local thermalization and collectivity in the system [13–15]. Hence, in the co-moving frame of the fluid cell, due to local thermalization, we take a Boltzmann distribution for the single quark or antiquark distribution, i.e.,

$$n_q^*(\boldsymbol{p}^*) = n_{\text{th}}(\boldsymbol{p}^*) = \frac{1}{4\pi m^2 T K_2(m/T)} e^{-E^*/T}, \quad (10)$$

where the superscript "$*$" denotes that these quantities are in the co-moving frame, K_2 is the Bessel function, m is the mass of the constituent quark (340 MeV for u or d quark and 500 MeV for strange quark), and $E^* = \sqrt{p^{*2} + m^2}$ is the energy of quark; T is the temperature of the system at hadronization (take as $T = 165$ MeV [16]).

For the joint momentum distribution of the quark and the antiquark produced in the same pair, we use the covariance coefficient ρ to describe the correlation between them. We recall that for a joint momentum distribution for a $q\bar{q}$ system, the covariance coefficient ρ is defined as $\rho = \text{cov}(\boldsymbol{p}_q, \boldsymbol{p}_{\bar{q}})/\text{var}(\boldsymbol{p}_{\bar{q}})$, where $\text{cov}(\boldsymbol{p}_q, \boldsymbol{p}_{\bar{q}}) \equiv \langle \boldsymbol{p}_q \cdot \boldsymbol{p}_{\bar{q}} \rangle - \langle \boldsymbol{p}_q \rangle \cdot \langle \boldsymbol{p}_{\bar{q}} \rangle$ and $\text{var}(\boldsymbol{p}_{\bar{q}}) \equiv \langle \boldsymbol{p}_{\bar{q}}^2 \rangle - \langle \boldsymbol{p}_{\bar{q}} \rangle^2$. We take the joint distribution for the $q\bar{q}$ system in the co-moving frame of the $q\bar{q}$ pair in the Cholesky factorization form, i.e.,

$$n_{q\bar{q}}^{\text{pair}*}(\boldsymbol{p}_q^*, \boldsymbol{p}_{\bar{q}}^*) = \frac{1}{2(1-\rho^2)^{3/2}} \left[n_{\text{th}}(\boldsymbol{p}_q^*) n_{\text{th}} \left(\frac{\boldsymbol{p}_{\bar{q}}^* - \rho \boldsymbol{p}_q^*}{\sqrt{1-\rho^2}} \right) \right.$$
$$\left. + n_{\text{th}}(\boldsymbol{p}_{\bar{q}}^*) n_{\text{th}} \left(\frac{\boldsymbol{p}_q^* - \rho \boldsymbol{p}_{\bar{q}}^*}{\sqrt{1-\rho^2}} \right) \right]. \quad (11)$$

The covariance parameter ρ describes the strength of the correlation. If $\rho = 0$, there is no correlation between the momentum distribution of the quark and that of the antiquark and we obtain the factorized form. For ρ very close to unity, we get a maximum correlation between the momentum of $\boldsymbol{p}_q$ and $\boldsymbol{p}_{\bar{q}}$, where the probability is nonzero only when $\boldsymbol{p}_q = \boldsymbol{p}_{\bar{q}}$. In general $-1 \leqslant \rho \leqslant 1$, and $\rho > 0$ means short-range compensation of q and $\bar{q}$ while $\rho < 0$ means the opposite.

The joint distribution $n_{q\bar{q}}^{\text{pair}}(\boldsymbol{p}_q, \boldsymbol{p}_{\bar{q}})$ in the laboratory frame is obtained from $n_{q\bar{q}}^{\text{pair}*}(\boldsymbol{p}_q^*, \boldsymbol{p}_{\bar{q}}^*)$. Here, we first make the Lorentz transformation ($\boldsymbol{\beta}$) from the co-moving frame of the fluid cell to the laboratory frame to obtain $n_{q\bar{q}}^{\text{pair}}(\boldsymbol{p}_q, \boldsymbol{p}_{\bar{q}}, \boldsymbol{\beta})$, then sum up the contributions from different fluid cells in the system with different collective velocities, i.e.,

$$n_{q\bar{q}}^{\text{pair}}(\boldsymbol{p}_q, \boldsymbol{p}_{\bar{q}}) = \int h(\boldsymbol{\beta}) n_{q\bar{q}}^{\text{pair}}(\boldsymbol{p}_q, \boldsymbol{p}_{\bar{q}}, \boldsymbol{\beta}) d^3 \beta, \quad (12)$$

where $h(\boldsymbol{\beta})$ is the so-called velocity function which corresponds to the velocity distribution of the fluid cell in the system.

The velocity function $h(\boldsymbol{\beta})$ is normalized to unity and can be decomposed into the longitudinal part h_L and the transverse part $h_\perp$. The longitudinal velocity β_z is usually replaced by the rapidity y. The azimuthal dependence is isotropic, we

integrate it out and obtain, $\int h(\boldsymbol{\beta})\,d^3\beta = h_L(y)h_\perp(\beta_\perp)\,dy d\beta_\perp$. This velocity function $h(\boldsymbol{\beta})$ determines, together with the momentum distribution of the quark and antiquark in the fluid cell, the single quark spectrum thus the inclusive momentum distribution of the hadrons after hadronization. In practice, it is parametrized by fitting the data for the hadron momentum distributions with the aid of hadronization models. According to the transparency observed in experiments [17], and because of that the observed rapidity spectra of hadrons show a roughly Gaussian shape in the full rapidity range [18], we take the transverse part as a uniform distribution between $[0, \beta_\perp^{\max}]$ and parametrize the longitudinal part in a Gaussian-like form,

$$h_L(y) = \frac{1}{2\sigma^{\frac{2}{a}}\Gamma(1+\frac{1}{a})} e^{-|y|^a/\sigma^2}. \tag{13}$$

The free parameters a, σ, and $\beta_\perp^{\max}$ are fixed using the data for the rapidity and the p_T spectra of hadrons. For example, in the following section of this paper, we just use the results obtained by fitting the data of rapidity and p_T spectra of final hadrons in central Au + Au collisions at $\sqrt{s_{NN}} = 200$ GeV [18,19] with the aid of the combination model for hadronization [20,21]. The results are $a = 2.40$, $\sigma = 2.54$, and $\beta_\perp^{\max} = 0.30$ for u and d newborn quarks and $a = 2.36$, $\sigma = 2.73$, and $\beta_\perp^{\max} = 0.34$ for strange quarks. The numbers of light and strange (anti)quarks and momentum distribution of net-quarks from the colliding nuclei have been fixed in Ref. [22].

B. Charge balance function of the bulk quark antiquark system

Having the joint momentum distribution functions, we can calculate the charge balance function in a straightforward way. In the following, we present the results in rapidity space for different transverse momentum intervals. In practice, the balance function in rapidity space is often rewritten as a function of the rapidity difference $\delta y = y_a - y_b$ between two particles in a limited window y_w, i.e.,

$$B_{ab}(\delta y | y_w) = \frac{1}{2}\left\{ \frac{N_{ba}(\delta y, y_w) - N_{aa}(\delta y, y_w)}{N_a(y_w)} + \frac{N_{ab}(\delta y, y_w) - N_{bb}(\delta y, y_w)}{N_b(y_w)} \right\}. \tag{14}$$

Since quarks of different flavors posses different electric charges, it is not straightforward to extend the definition of the the electric charge balance function given by Eq. (1) or Eq. (14) to the quark-antiquark system. There is no direct extension of Eq. (14) to such cases. We have many different possibilities at the quark level, e.g.,

$$B_q^{(c1)}(\delta y | y_w) = -\frac{1}{2N_f}\sum_{a,b} \frac{e_a e_b N_{ab}(\delta y, y_w)}{e_a^2 N_a(y_w)}, \tag{15}$$

$$B_q^{(c2)}(\delta y | y_w) = -\frac{1}{2N_f}\sum_{a,b} \frac{\text{sgn}(e_a e_b) N_{ab}(\delta y, y_w)}{N_a(y_w)}, \tag{16}$$

where both a and b run over all the quarks and the antiquarks, N_f is the number of flavor involved. We can also define it as

$$B_q^{(c3)}(\delta y | y_w) = -\frac{1}{2}\left\{ \frac{\sum_{a,b}\text{sgn}(e_a e_b)N_{ba}(\delta y, y_w)}{\sum_a N_a(y_w)} + \frac{\sum_{a,b}\text{sgn}(e_a e_b)N_{ab}(\delta y, y_w)}{\sum_b N_b(y_w)} \right\}, \tag{17}$$

where $a = u$, $\bar{d}$, or $\bar{s}$ while $b = \bar{u}$, d, or s represent the positively and negatively charged particles, respectively. We may also define the baryon number balance function for the quark-antiquark system instead, which is given by

$$B_q^{(b1)}(\delta y | y_w) = -\frac{1}{2N_f}\sum_{a,b} \frac{B_a B_b N_{ab}(\delta y, y_w)}{B_a^2 N_a(y_w)}, \tag{18}$$

where the summations over a and b run over all different flavors of quarks and those of antiquarks, and B_a and B_b stand for the baryon numbers. We can also define it as

$$B_q^{(b2)}(\delta y | y_w) = -\frac{1}{2}\left\{ \frac{\sum_{a,b} B_a B_b N_{ba}(\delta y, y_w)}{\sum_a B_a^2 N_a(y_w)} + \frac{\sum_{a,b} B_a B_b N_{ab}(\delta y, y_w)}{\sum_b B_b^2 N_b(y_w)} \right\}, \tag{19}$$

where a denotes all the quarks of different flavors and b all the antiquarks of different flavors, respectively. All these definitions satisfy $\int d\delta y\, B_q(\delta y | y_w) = 1$.

We note that so far as the kind of correlations between the momentum distributions of the quarks and that of the antiquarks described in the working model presented in Sec. II A are concerned, all these definitions do not make much difference. More precisely, in the working model presented in Sec. II A, only a correlation between the momentum of the quark and that of the antiquark from the same $q\bar{q}$ pair is introduced as given by Eq. (11). There is no correlation between the quarks and antiquarks from different pairs and there is no difference between different flavors. In this case, all the definitions given by Eqs. (15)–(19) are equivalent in the sense that they are all different suppositions of the correlations given by Eq. (11) for different flavors and Eq. (11) does not distinguish between different flavors. The only differences come from the net-quark contributions where no strange quark exists. For comparison, we made the calculations using the different definitions Eqs. (15)–(19) and the results are indeed similar. In the following part of this section, we show the results obtained by using Eq. (17).

We first study the case where $\rho = 0$. In this case, there is no correlation between the momentum distribution of the quarks and antiquarks. The balance is obtained only from the global flavor compensation of the new created quarks and antiquarks. This is also the minimum compensation in the produced system. In Fig. 1(a), we show the results of $y_w = 1$ for different rapidity positions with transverse momentum $p_\perp$ integrated. In Fig. 1(b), we show the results for $\rho = 0.5$ and a comparison of the results for different values of ρ is given in Fig. 1(c).
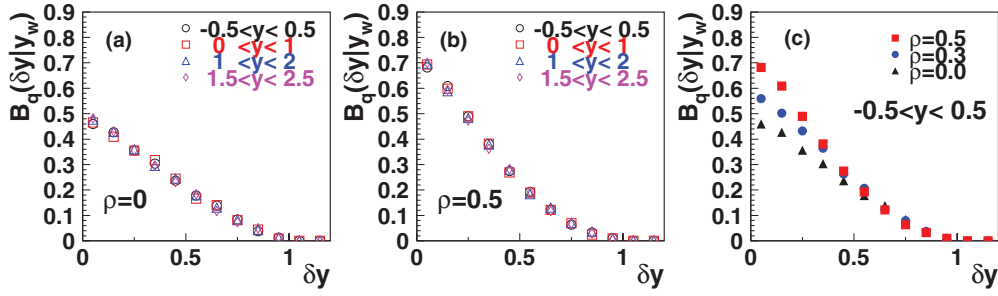
FIG. 1. (Color online) The electric charge balance function $B_q(\delta y|y_w)$ for the bulk quark system for the same window size as a function of δy at the covariance coefficient $\rho = 0$ in (a) and $\rho = 0.5$ in (b), respectively. A comparison of the results at different values of ρ is shown in (c).

From the results, we see that in all cases, also for $\rho = 0$, the balance function $B_q(\delta y|y_w)$ decrease with increasing δy showing a local compensation of the electric charge in the rapidity space for the bulk quark system. It is also clear that $B_q(\delta y|y_w)$ decreases faster with increasing δy for a larger value of ρ indicating stronger local charge compensation. We also see that $B_q(\delta y|y_w)$ does not change much for different rapidity window with the same window size showing the longitudinal boost invariance. This holds for different values of the variance coefficient ρ.

The existence of the approximate boost invariance for the charge balance function for the bulk quark system can easily be understood. We note that by looking at the different rapidity window in the case that the window size is much smaller than the total rapidity range of the bulk quark system, we are in fact looking at different fluid cells. Since we do not differentiate these fluid cells in any significant way, the results should be similar. This results in similar charge balance function as indicated by the calculated results shown in Fig. 1. In other words, the boost invariance of the charge balance function just reflects the homogeneity of the fluid cell at hadronization in different rapidity windows.

We continue to study the dependence of the balance function $B_q(\delta y|y_w)$ on the window size and/or transverse momentum. In Fig. 2(a), we show $B_q(\delta y|y_w)$ in the different rapidity positions with the same window size $y_w = 1$ and in Fig. 2(b), we show $B_q(\delta y|y_w)$ at different window sizes $y_w = 1, 2, 3, 4$. We see that $B_q(\delta y|y_w)$ varies with window size and becomes flatter with increasing window size. This qualitative feature is naturally expected from the definition since the balance function is normalized to unity but the range

of the allowed values of δy becomes larger for the larger window size. This effect can be eliminated by scaling the balance function $B_q(\delta y|y_w)$ with the factor $1 - \delta y/|y_w|$ as suggested in Ref. [2], i.e., we study the scaled balance function,

$$B_s(\delta y) = \frac{B(\delta y|y_w)}{1 - \delta y/y_w}. \qquad (20)$$

In Fig. 2(c), we show the results obtained for the scaled $B_s(\delta y)$ of the bulk quark system. We see clearly that the scaled balance functions fall on one curve showing that they are independent of the size and position of rapidity window. For comparison, we also present the balance function in the full rapidity region (open cross) for the case that the net charge of the system is taken to be zero. We see that the result is also consistent with those for the limited rapidity windows so far as the scaled balance function is studied. This is very nice feature since it suggests that the scaled balance function for particles in the limited rapidity window can indeed be regarded as an example for the charge balance function of the system.

We emphasize that these properties of the balance functions of the bulk quark system are results of the momentum distributions of the quarks and antiquarks in the system. These distributions including the correlations given by Eq. (11) are results of the local thermalization and collectivity for the system produced in relativistic heavy ion collisions in the hydrodynamic theory. These qualitative features for the charge balance functions for the bulk quark system before hadronization are consistent with those for the final hadrons as observed by STAR Collaboration at RHIC [12]. We also note that these properties are mainly determined by the correlations given by Eq. (11). They only depend weakly on the single
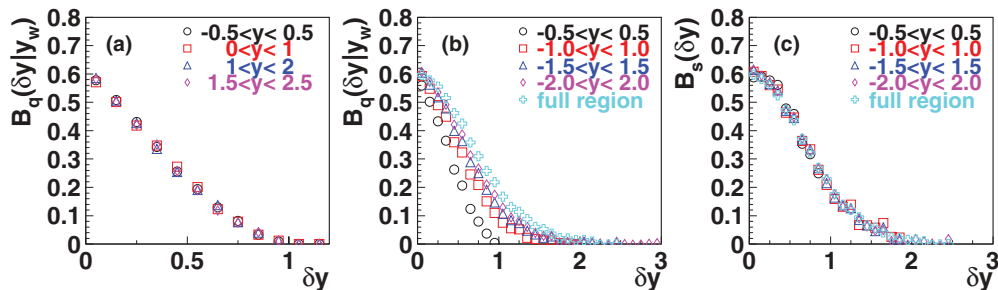

FIG. 2. (Color online) The p_T-integrated $B_q(\delta y|y_w)$ of the bulk quark system at different rapidity positions with same (a) and different (b) window sizes, as well as the $B_s(\delta y)$ (c). Correlation coefficient ρ is taken to be 0.3.
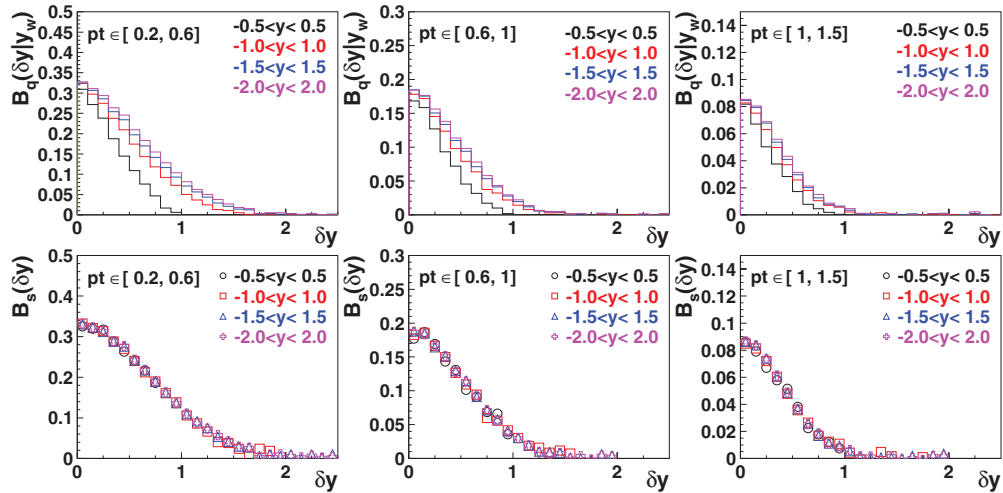
FIG. 3. (Color online) The $B_q(\delta y | y_w)$ of bulk quark system (top panels) at different rapidity positions with different window sizes as well as the $B_s(\delta y)$ (bottom panels) in the different p_T (GeV/c) ranges. Correlation coefficient ρ is taken to be 0.3.

quark or antiquark momentum distribution itself. We have also made calculations using the Fermi-Dirac distribution instead of the Boltzmann distribution given in Eq. (10) for the single quark or antiquark momentum distribution. For the reasons mentioned above and also because E^* is much larger than the temperature T so that the difference between the corresponding Fermi-Dirac and the Boltzmann distribution is small, the obtained balance functions are essentially the same in the two cases. The difference is usually less than 1%.

In Fig. 3, we show $B_q(\delta y | y_w)$ and $B_s(\delta y)$ in different rapidity windows and in the different p_T ranges. We clearly see that the scaling properties of the balance function still hold in the different p_T ranges. We can also see that the width of the scaled balance function decreases with increasing p_T. This is because, in general, the quarks and antiquarks with larger p_T come from the fluid cell with larger transverse flow, which results in a smaller longitudinal rapidity interval and hence smaller width for the balance function. Such a feature is consistent with the observation in central Au + Au collisions at $\sqrt{s_{NN}} = 200$ GeV [12].

III. CHARGE BALANCE FUNCTIONS OF THE HADRON SYSTEM

With the momentum distribution functions of the bulk quark system discussed in the last section, we study the charge balance functions of hadrons produced in the hadronization of this system. We compare the results obtained for the directly produced hadrons and those of the final state hadrons with those for the quarks and antiquarks to study the influence of the hadronization and resonance decay on the balance functions.

We describe the hadronization of the bulk quark system with the (re)combination or coalescence mechanism. Such a hadronization mechanism is tested by various data and is implemented in different forms such as the quark recombination model [23,24], the parton coalescence model [25,26], and the quark combination mode (SDQCM) [20,21]. All these models

are tested against the various features of the hadrons produced in heavy ion collisions at high energies. Here, in this paper, we use SDQCM [20,21] for our calculations since this model takes the exclusive description and is implemented by a Monte Carlo program so that can be apply to calculate the balance functions for the directly produced hadrons as well as the final hadrons after the resonance decays in a very convenient way. Also, this model guarantees that mesons and baryons exhaust all the quarks and antiquarks in the deconfined color-neutral system at hadronization.

We note that the main purpose here is to study the influence of the hadronization and resonance decay on the charge balance function by comparing the results obtained before and after hadronization, we only consider the hadronization of the bulk quark-antiquark system in the combination mechanism but do not consider the gluon influence in the following. Gluon contribution might have significant influence on the hadronization and charge balance function as well. However, it is still unknown how to take such contribution into account in the combination mechanism and such study should be an interesting topic in the future.

A. Charge balance functions in rapidity space

We insert the momentum distributions including the correlations given by Eq. (11) to determine the momenta of the quarks and antiquarks before hadronization. We then apply the quark combination rules as implemented in the Monte Carlo program of SDQCM [21] to calculate the momentum distribution of the directly produced hadrons. Those resonances will decay accordingly and the momentum distributions are simulated also in the program by using the material from the particle data group [27].

In Fig. 4, we show the results for the p_T-integrated balance functions for the directly produced hadrons. Here, in Fig. 4(a), we see the results in different rapidity windows with the same width $y_w = 1$, while in Fig. 4(b) and 4(c), we see the results at different window sizes as well as the scaled function $B_s(\delta y)$.
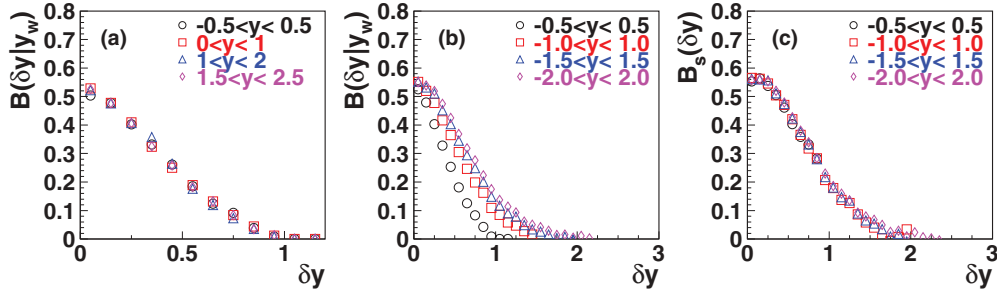
FIG. 4. (Color online) The p_T-integrated $B(\delta y|y_w)$ of initial hadron system at different rapidity positions with same (a) and different (b) window sizes, as well as the $B_s(\delta y)$ (c). Correlation coefficient ρ is taken to be 0.3.

In Fig. 5, we show the corresponding results in different p_T ranges.

From these results, we see that both the longitudinal boost invariance and rapidity scaling for the balance functions are held for the hadrons directly produced in the quark combination mechanism, either for the p_T-integrated quantities or those for different p_T ranges. This is in fact not surprising because the formation of hadrons in this hadronization mechanism is realized by the combination of two or three nearest quarks/antiquarks in momentum space. This means that the combination happens locally and does not destroy the locality nature of the charge balance of the system.

We further study the resonance decay contributions by calculating the balance functions for the final hadrons where decays of the resonances are taken into account. We show the corresponding results in Figs. 6 and 7.

From Figs. 6 and 7, we see that both the boost invariance in rapidity space and the scaling property are still preserved after the contributions from the resonance decays are taken into account. Together with those results given in Figs. 4 and 5, these results show clearly, although there are definitely influences from hadronization and resonance decay on the form of the charge balance functions, these effects do not significantly influence the boost invariance and the scaling in rapidity space.

The influences from hadronization and resonance decay to the balance function can be studied more quantitatively by calculating the averaged width of the balance function, which is defined as

$$\langle \delta y \rangle = \frac{\int_0^{y_w} B(\delta y|y_w)\, \delta y\, d\delta y}{\int_0^{y_w} B(\delta y|y_w) d\delta y}. \qquad (21)$$

We note that the averaged width $\langle \delta y \rangle$ is in general a characterizing quantity describing the radius of charge balance of the system. For the final hadron system in heavy ion collisions, it can be sensitive to different effects such as delayed hadronization or hadron freeze-out [1,28], possibly highly localized charge balance at freeze-out [29], transverse flow [3,31], multiplicity effect [30,32], and hadronic weak decay. Here, by comparing the results for the balance functions of the quark-antiquark system with those for the initial hadrons and those for the final hadrons, we can study the magnitudes of the influences of hadronization and those from resonance decay.

In Fig. 8(a), we show the results for the averaged width $\langle \delta \eta \rangle$ of the balance function for the directly produced hadrons as the function of ρ, compared with that for the quarks and antiquarks and that for the final hadrons. Here, we show the results for pseudorapidity η in order to compare with the experimental data now available [11]. We choose also the same pseudorapidity and p_T regions as the experiments [11],
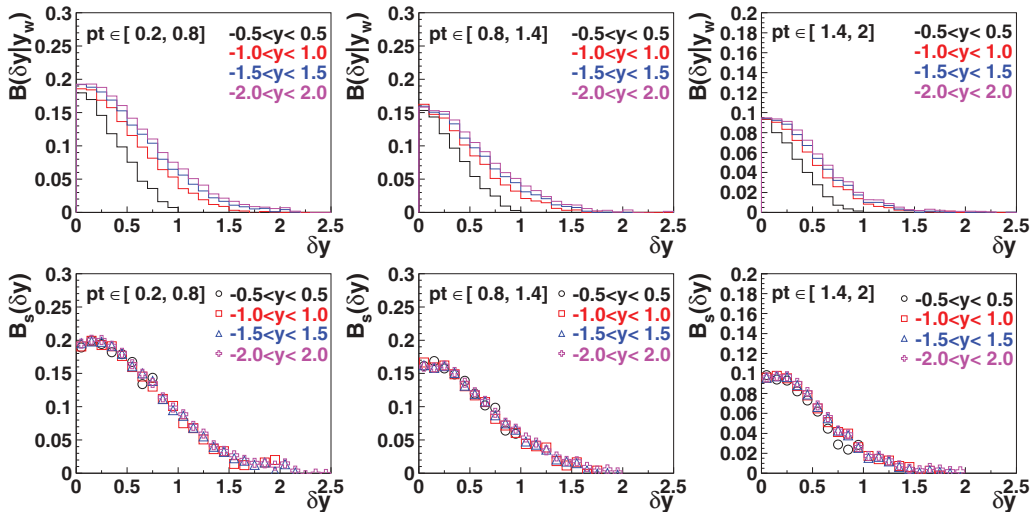

FIG. 5. (Color online) The $B(\delta y|y_w)$ of initial hadron system (top panels) at different rapidity positions with different window sizes as well as the $B_s(\delta y)$ (bottom panels) in the different p_T (GeV/c) ranges. Correlation coefficient ρ is taken to be 0.3.
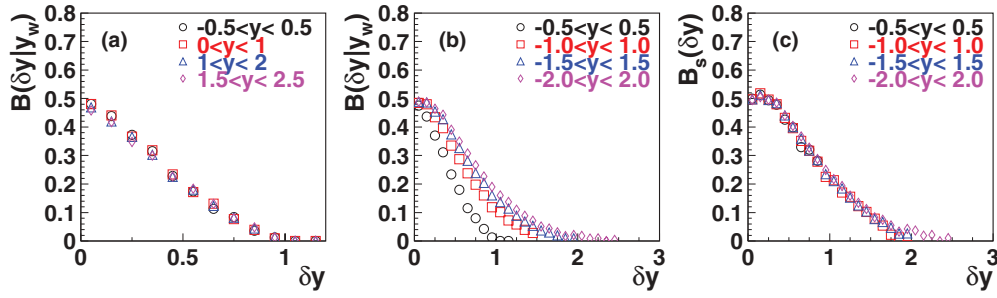
FIG. 6. (Color online) The p_T-integrated $B(\delta y | y_w)$ of final hadron system at different rapidity positions with same (a) and different (b) window sizes, as well as the $B_s(\delta y)$ (c). Correlation coefficient ρ is taken to be 0.3.

i.e., $|\eta| < 1$, $0.1 \leqslant |\delta \eta| \leqslant 2.0$, and $0.2 < p_T < 2.0$ GeV/c. In Fig. 8(a), the data of $\langle \delta \eta \rangle$ in central Au+Au collisions at $\sqrt{s_{NN}} = 200$ GeV [11] is shown as a band area. We see clearly that, in all three cases, the averaged width $\langle \delta \eta \rangle$ decreases with the increasing ρ. We see also that the $\langle \delta \eta \rangle$ for the directly produced hadron system decreases with the increasing ρ in exactly the same way as that for the bulk quark system does. The difference between $\langle \delta \eta \rangle$ for the directly produced hadron system and that for the bulk quark system is almost a constant 0.04 for all the different values of ρ. This is because, as mentioned above, the combination of quark(s) and/or antiquark(s) in neighbor areas does not change the electric charge balance in any essential way. However, the formation of electrically neutral hadrons may delay the charge balance in momentum space. We take a quark and an antiquark from a given $q\bar{q}$ pair as an example. As given by Eq. (11), their momentum distributions possess a correlation measured by the covariance coefficient ρ. If both of them enter into the respectively charged hadrons in the combination process, the correlation will pass to the hadronic level. However, if one of them enters into an electrically neutral hadron, the correlation will be lost in the charged hadrons. This will decrease the local charge balance at the hadron level.

From Fig. 8(a), we also see that the resonance decay contributions change $\langle \delta \eta \rangle$ significantly. It is also interesting to see that these contributions strengthen the local charge balance for relatively small values of ρ but weaken the balance for larger values of ρ. This indicates that the decay contributions dilute the balance functions quite significantly. To see where these different behaviors come from, we calculate the averaged width $\langle \delta y \rangle$ for those hadrons from resonance decay separately. We note that the influence of resonance decay to the charge balance function is in general different for hyperon decay from that for vector-meson decay. The decay of the hyperons such as $\Lambda \rightarrow p\pi$ and $\Xi^0 \rightarrow \Lambda\pi$ produces a pair of charged daughter particles with quite narrow rapidity interval, e.g., about one-third for $\Lambda \rightarrow p\pi$ and $\Xi^0 \rightarrow \Lambda\pi$, due to the small amount of energy released in the decay process. This leads also to a smaller $\langle \delta \eta \rangle$ for the charge balance function. However, in vector meson decay such as $\rho^0 \rightarrow \pi^+\pi^-$ and $K^{*0} \rightarrow K^+\pi^-$, the energy released is much larger leading to a much larger rapidity difference between the daughter particles, e.g., up to 1.7 for $\rho^0 \rightarrow \pi^+\pi^-$ and 1.3 for $K^{*0} \rightarrow K^+\pi^-$ in the rest frame of parent particle. To study this effect in a more quantitative manner, we calculate the averaged width $\langle \delta \eta \rangle$ of the balance function only for the daughter particles from
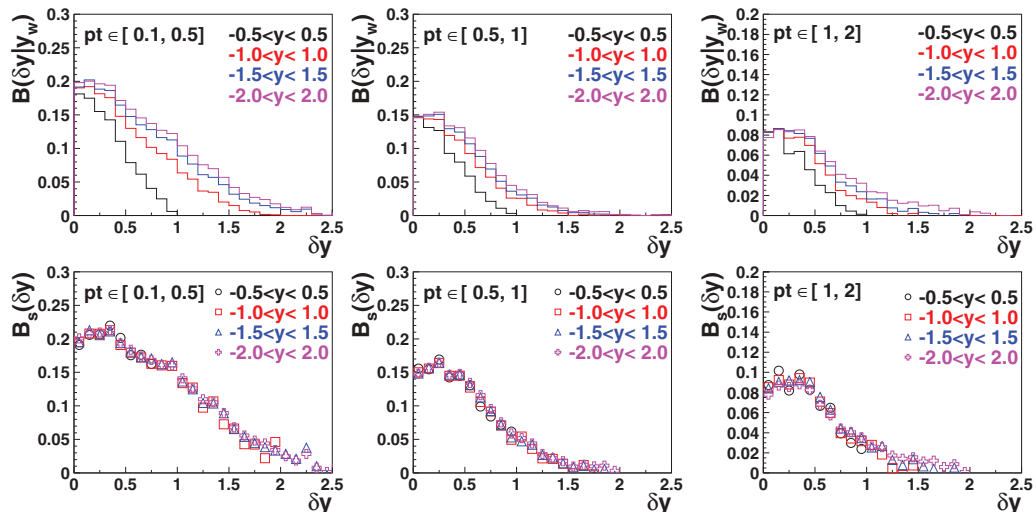

FIG. 7. (Color online) The $B(\delta y | y_w)$ of final hadron system (top panels) at different rapidity positions with different window sizes as well as the $B_s(\delta y)$ (bottom panels) in the different p_T (GeV/c) ranges. Correlation coefficient ρ is taken to be 0.3.
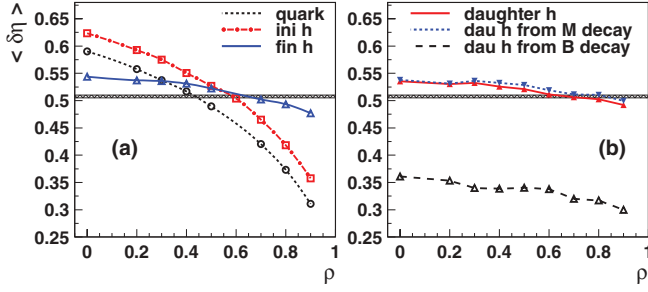
FIG. 8. (Color online) In (a), we see the averaged widths ⟨δη⟩ of the balance functions for the quark and antiquark, the directly produced and the final hadron systems as functions of ρ. In (b), we see the averaged widths ⟨δη⟩ of the balance functions for the daughter hadrons from all the resonance decays, those for the daughter hadrons from the meson decays and those from the baryon decays, respectively. The band area represents the experimental of ⟨δη⟩ for charged particles in central Au+Au $\sqrt{s_{NN}} = 200$ GeV [12].

baryon or meson decay, respectively. The results are shown in Fig. 8(b). Here, we see clearly that the averaged width ⟨δη⟩ for the daughter particles from baryon decay is indeed much smaller than those from meson decay. We see also that the charge balance for the daughter particles from baryon decays is dominated by the decay effect which leads to an averaged width of about one-third. However, for those from meson decays, the charge balance is dominated by the effect from the mother particles.

B. Charge balance in the azimuthal direction

The charge balance in the azimuthal direction for hadrons in high energy heavy ion collisions can be sensitive to jet production. Experimental studies have already been carried out by the STAR Collaboration for hadrons of different p_T regions [11]. It is thus also interesting to see how the charge

balance function behaves for the bulk quark matter system and the resulting hadrons.

The balance function of hadrons in the azimuthal direction is defined similarly to that in rapidity,

$$B_{ba,azi}(\delta\phi, \phi) = \frac{1}{2}\left\{ \frac{N_{ba}(\delta\phi,\phi) - N_{aa}(\delta\phi,\phi)}{N_a(\phi)} + \frac{N_{ab}(\delta\phi,\phi) - N_{bb}(\delta\phi,\phi)}{N_b(\phi)} \right\}, \quad (22)$$

where, the quantity $N_{ba}(\delta\phi, \phi)$ is defined as the number of pairs of particles with the particle a flying at an angle ϕ (measured with respect to the reaction plane) and the particle b at an angle between ϕ and $\phi + \delta\phi$. In the following we study the azimuthally averaged balance function:

$$B_{ab,azi}(\delta\phi) = \int_0^{2\pi} d\phi\, B_{ab}(\delta\phi, \phi). \quad (23)$$

Having the Monte Carlo program at hand, the extension of the calculations mentioned above to azimuthal direction is straightforward. We show the results obtained for the quark, the directly produced hadron, and the final hadron system at different ρ values in Fig. 9. Comparison with the available data [11] is also given in the figure.

From the results for the bulk quark system [Fig. 9(a)], we see clearly that the dependence of the quark charge balance function on the variance parameter ρ is quite obvious. For ρ close to unity, the momentum of the quark and that of the antiquark produced in the pair are closely correlated, and we see a sharp peak at δφ = 0. For ρ = 0, there is no correlation and the balance function is almost a flat function showing only the influence from the global charge compensation.

Comparing the results in Fig. 9(b) with those in Fig. 9(a), we see that the charge balance functions in the azimuthal direction for the directly produced hadron system are slightly broader than the corresponding results for the quark system, showing a
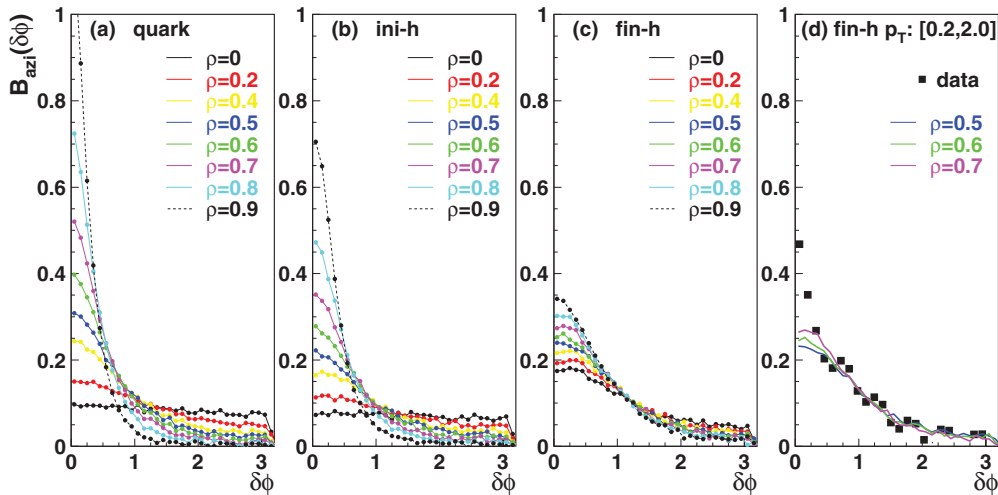

FIG. 9. (Color online) Balance function $B_{azi}(\delta\phi)$ of the quark-antiquark system (a), the directly produced hadron system (b), and the final hadron system (c) as functions of δφ in the pseudorapidity region $-1 < \eta < 1$ and $0.2 < p_T < 2.0$ GeV/c. A comparison of the results for the final hadron system at ρ = 0.5, 0.6, and 0.7 and the experimental data for all charged particles with $0.2 < p_T < 2.0$ GeV/c in central Au + Au collisions at $\sqrt{s_{NN}} = 200$ GeV in Ref. [11] is given in (d).

slightly loose correlation. This is similar to the case in rapidity space studied in the last subsection. However, the influences from the resonance decays are quite significant in the azimuthal direction. We see quite significant differences between the results for the final hadrons and the corresponding results for the hadron system before resonance decay. We see in particular that the very much pronounced peak at $\delta\phi = 0$ is smoothed by the decay influences. This is also obvious since such a strong correlation can be destroyed by the resonance decay because of the transverse momentum conservation in the decay processes. From Fig. 9(c), we see that the data [11] are well be described except for the peak at $\delta\phi = 0$. This peak could be an indication of jet contribution which is not included in our calculations.

local thermalization and collectivity. A correlation between the momentum distribution of the quark and that of the antiquark is introduced if they are from the same new produced $q\bar{q}$ pair and the correlation strength is described by the variance coefficient ρ. Our results show that the charge balance functions for the bulk quark system have the longitudinal boost invariance and the scaling behavior in rapidity space. Such properties are preserved by the subsequent hadronization via combination mechanism and the resonance decay, although both hadronization and resonance decay can influence the width of the balance function. With the same inputs, we also studied the balance function in the azimuthal direction.

IV. SUMMARY

In summary, we have calculated the charge balance functions of the bulk quark system before hadronization, those for the directly produced and the final hadron system in relativistic heavy ion collisions. The momentum distributions for the quarks and the antiquarks in the bulk quark system are taken as determined in the hydrodynamic picture with

[1] S. A. Bass, P. Danielewicz, and S. Pratt, Phys. Rev. Lett. **85**, 2689 (2000).
[2] S. Jeon and S. Pratt, Phys. Rev. C **65**, 044902 (2002).
[3] A. Bialas, Phys. Lett. B **579**, 31 (2004).
[4] S. Cheng, S. Petriconi, S. Pratt, M. Skoby, C. Gale, S. Jeon, V. T. Pop, and Q.-H. Zhang, Phys. Rev. C **69**, 054906 (2004).
[5] P. Bożek, W. Broniowski, and W. Florkowski, Acta Phys. Hung. A **22**, 149 (2005).
[6] N. Li, Z. M. Li, and Y. F. Wu, Phys. Rev. C **80**, 064910 (2009).
[7] S. Pratt, Phys. Rev. C **85**, 014904 (2012).
[8] C. Alt et al. (NA49 Collaboration), Phys. Rev. C **71**, 034903 (2005).
[9] C. Alt et al. (NA49 Collaboration), Phys. Rev. C **76**, 024914 (2007).
[10] J. Adams et al. (STAR Collaboration), Phys. Rev. Lett. **90**, 172301 (2003).
[11] M. M. Aggarwal et al. (STAR Collaboration), Phys. Rev. C **82**, 024905 (2010).
[12] B. I. Abelev et al. (STAR Collaboration), Phys. Lett. B **690**, 239 (2010).
[13] P. F. Kolb and U. Heinz, arXiv:nucl-th/0305084; Invited review in Quark Gluon Plasma 3, edited by R. C. Hwa and X. N. Wang (World Scientific, Singapore, 2004), p. 634.
[14] J. Adams et al. (STAR Collaboration), Nucl. Phys. A **757**, 102 (2005).
[15] K. Adcox et al. (PHENIX Collaboration), Nucl. Phys. A **757**, 184 (2005).
[16] F. Karsch, Nucl. Phys. A **698**, 199 (2002).
[17] I. G. Bearden et al. (BRAHMS Collaboration), Phys. Rev. Lett. **93**, 102301 (2004).
[18] I. G. Bearden et al. (BRAHMS Collaboration), Phys. Rev. Lett. **94**, 162301 (2005).
[19] S. S. Adler et al. (PHENIX Collaboration), Phys. Rev. C **69**, 034909 (2004).
[20] Q. B. Xie and Z. T. Liang, in Multiparticle Production Proceedings of the SHANDONG Workshop, edited by R. C. Hwa and Q. B. Xie (World Scientific, Singapore, 1987), p. 469; Q. B. Xie and X. M. Liu, Phys. Rev. D **38**, 2169 (1988).
[21] F. L. Shao, Q. B. Xie, and Q. Wang, Phys. Rev. C **71**, 044903 (2005).
[22] J. Song, F. L. Shao, and Q. B. Xie, Int. J. Mod. Phys. A **24**, 1161 (2009).
[23] R. J. Fries, B. Müller, C. Nonaka, and S. A. Bass, Phys. Rev. Lett. **90**, 202303 (2003).
[24] R. C. Hwa and C. B. Yang, Phys. Rev. C **67**, 034902 (2003).
[25] V. Greco, C. M. Ko, and P. Lévai, Phys. Rev. Lett. **90**, 202302 (2003).
[26] D. Molnár and S. A. Voloshin, Phys. Rev. Lett. **91**, 092301 (2003).
[27] C. Amsler et al. (Particle Data Group), Phys. Lett. B **667**, 1 (2008).
[28] J. H. Fu, J. Phys. G: Nucl. Part. Phys. **38**, 065104 (2011).
[29] S. Schlichting and S. Pratt, Phys. Rev. C **83**, 014913 (2011).
[30] J. X. Du, N. Li, and L. S. Liu, Phys. Rev. C **75**, 021903(R) (2007).
[31] P. Bożek, Phys. Lett. B **609**, 247 (2005).
[32] M. R. Atayan et al. (EHS/NA22 Collaboration), Phys. Lett. B **637**, 39 (2006).